A Compact, Self-Aligned Focusing Schlieren System

BRETT F. BATHEL[1,*] AND JOSHUA M. WEISBERGER[1]

[1] Advanced Measurements and Data Systems Branch, NASA Langley Research Center, Hampton, Virginia, 23681, USA
[*] Corresponding author: brett.f.bathel@nasa.gov

Compiled June 4, 2021

A novel compact, self-aligned focusing schlieren system is presented that eliminates the need for a separate source grid and cutoff grid. A single grid element serves to both generate a projected source grid onto a retroreflective background, and to act as the cutoff grid for the reflected light. This is made possible by manipulating the polarization of the light through the system. The use of only a single grid element eliminates the need to create a cutoff grid that is perfectly matched and scaled to the source grid, and removes the need to align the source and cutoff grids to each other. The sensitivity to density objects is adjustable with the use of a polarizing prism. Images obtained with this system show similar operation to existing focusing schlieren systems, but with much reduced complexity and setup time. Images taken with acrylic windows placed normal to the optical axis further demonstrate the system's utility for wind tunnel measurements.

http://dx.doi.org/10.1364/ao.XX.XXXXXX

1. INTRODUCTION

Schlieren imaging is routinely used as a flow visualization tool that is sensitive to density gradients. A typical conventional schlieren system collimates light from a small, point-like source using a field focusing optic (either a high-quality parabolic mirror or a lens) and passes this collimated light through the flowfield of interest. A second field focusing optic placed on the opposite side of the flowfield images the original light source at a point. A knife-edge located at this point is placed such that it blocks a portion of the image of the light source, with the remainder of the light passing through to a camera sensor. Any gradient in density that exists between the two field optics results in a refractive index gradient that diverts some of the rays of light in the light column. These diverted rays ultimately either terminate on, or pass by, the knife-edge. The resulting image captured by the camera sensor then consists of light and dark regions that correspond to structures of varying density in the flowfield. A thorough description of typical conventional schlieren imaging systems can be found in Ref. [1].

While the qualitative images schlieren can provide are useful for flow characterization, they represent the entire path-integrated density gradient field that exists between the two field focusing optics. Thus, every density gradient feature present in the field-of-view is captured in the resulting image, including features that are not pertinent to the flow of interest. Examples include non-relevant flow features, wind tunnel window scratches or chips, wind tunnel plenum or HVAC thermals, and wind tunnel wall boundary layer turbulent structures. These obscure relevant flow features and complicate their interpretation. The field-of-view of a conventional schlieren system is also limited to the clear aperture/diameter of the field focusing optics.

The focusing schlieren technique was developed to address the limiting characteristics of the conventional schlieren system; it can significantly reduce the influence of non-pertinent flow features and can provide larger fields-of-view. Typical focusing schlieren systems use a source grid placed on one side of the density object, which is then imaged with a lens onto a matching cutoff grid on the other side of the density object. Source grids usually consist of either a one-dimensional pattern of equally-spaced parallel line pairs or a two-dimensional regular pattern of shapes. The cutoff grid must consist of a scaled duplicate of the source grid and can be challenging to create. By adjusting the offset of the cutoff grid relative to the image of the source grid, the sensitivity of the instrument to density gradients present between the source grid and imaging lens can be tuned (similar to adjusting the knife-edge insertion in a conventional system). For this type of setup, the numerous high-intensity/bright regions of the source grid effectively serve as the light sources for a number of conventional schlieren systems whose paths all intersect a common region that contains the flow feature of interest. This method of operation, in effect, defocuses the contribution of features that occur away from this common region in the final image.

The most common design is the modern large-field focusing schlieren system described by Weinstein [2, 3] and Settles [1]. In these systems, a light source back-illuminates the source grid, with a Fresnel lens placed between the two in order to better direct light into the camera lens and improve brightness. The source grid is imaged onto the cutoff grid with a field lens, and the resulting focused schlieren image captured at the image plane by a camera. Placement of the source and cutoff grids relative to the field lens are readily determined using the thin lens equation, as is the placement of the schlieren object and image plane. An alternative source grid consisting of patterned retroreflective material was used by Heineck [4], with illumination provided by coupling light onto the optical axis via a beam splitting plate, and the resulting image of the source grid was incident on a matched cutoff grid. This system is useful when

cross-tunnel optical access is not available, and when larger fields-of-view are required than provided by a Fresnel lens. Another retroreflective system has been demonstrated, where the source grid is instead projected onto the screen and imaged onto a separate matched cutoff grid [3, 5]. Recent advancements in digital display technology have enabled source grids to be tailored to the cutoff grid. The use of a digital projection system was described in Ref. [6] to project an image of a digital source grid onto a screen. Digital display devices such as LCD and LED monitors (either backlit or self-illuminating) have been successfully used to generate source grids matched to a cutoff grid [6–8].

In all the aforementioned focusing schlieren systems, a separate source and cutoff grid are required, resulting in two major limitations. First, it is difficult to create or obtain a cutoff grid that is well-matched and properly scaled to the imaged source grid. Second, nearly perfect alignment between the cutoff grid and the imaged source grid is required. Film-based cutoff grids are developed from the negative of the source grid, but must then be installed in the system and meticulously aligned to the image of the source grid. Optical aberrations in the imaging optics can degrade the quality of the images, since the film-based cutoff grid would no longer be an exact match of the imaged source grid. To avoid this degradation, the film would need to be developed in the exact setup of the installed system. Digital display methods can alleviate some of the difficulty in obtaining precise alignment between the source and cutoff grids, but they are restricted to lower-speed flows/fluctuations as light from the output of commercially-available digital displays is limited, and they still require a computer to match the displayed source grid to a physical cutoff grid. Transparent digital LCD displays with pulsed laser back-illumination do allow for high-speed measurements, although this (along with conventional digital displays) requires the use of bulky display equipment that may not be conducive to tests in space-restricted environments (e.g. wind tunnels) [8, 9]. The colinear illumination projection systems described in Refs. [3–5] also present significant challenges when used near a window, as back-reflections can cause intense hot spots to appear that adversely affect system performance [3, 7].

Here, we present a novel compact, inherently self-aligned focusing schlieren system that eliminates the need for a separate source grid and cutoff grid. The complexity of the experimental setup is greatly reduced, and by eliminating one of the two grids, no effort is required to precisely match and align the source to the cutoff grid. The system manipulates the polarization state of the light through the optics to provide sensitivity adjustment, and also eliminates glare and back-reflections from windows that are often present in wind tunnel facilities, even at normal incidence.

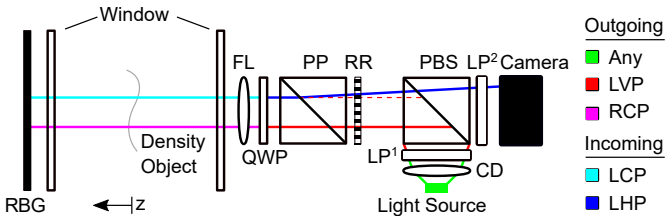

Fig. 1. Schematic of compact, self-aligned focusing schlieren concept.

A schematic of the concept is shown in Fig. 1. The instrument first directs unpolarized light from a light source towards a polarizing beam splitter (PBS). Note that the light source can also possess any polarization state without limitation. An optional condenser lens with a diffuser (CD) can be used to diffuse and loosely focus the light to improve the resulting image brightness. An optional linear polarizer (LP^1) can be placed between the CD and the PBS, since linear polarizers often have a higher extinction ratio than polarizing beam splitters. The PBS then reflects linearly-vertically-polarized (*lvp*) light such that it is coupled onto the optical axis of the instrument, while simultaneously passing through linearly-horizontally-polarized (*lhp*) light. The *lvp*-light passes through a transparent slide with an opaque grid pattern (e.g. a Ronchi ruling). The light, now spatially filtered by the grid element, passes through a polarizing prism (PP) that is oriented such that the *lvp*-light passes through unrefracted. Next the *lvp*-light passes through a quarter-wave plate (QWP) that alters the polarization state from *lvp* to right-circularly-polarized (*rcp*). This *rcp*-light passes through a field lens (FL) that is used to project the image of the RR onto a retroreflective background (RBG). While the light propagates towards the RBG, it passes through the density object. In many wind tunnel facilities, windows may also be present on either side of this density object.

Upon reflection off of the RBG, the light's polarization state is changed to left-circularly-polarized (*lcp*) and it again passes through the density object and any windows that may be present. An increase in sensitivity is achieved by double-passing the light through the density object in a manner similar to single-mirror coincident schlieren systems [1]. The light is then re-imaged by the FL and the QWP modifies the polarization state from *lcp* to *lhp*. As the light now passes through the PP, it is refracted by a small angle as a result of the differing refractive index that the orthogonal linear polarization states encounter within the PP. The re-imaged grid projection is then incident on the original grid RR with a small offset, providing partial cutoff of the re-imaged grid projection and therefore increased sensitivity to the density object. The *lhp*-light is then transmitted by the PBS and an imaging sensor is placed at the image focal plane. Note that an optional second linear polarizer (LP^2) may be placed in front of the image sensor to further improve image contrast (increased extinction ratio). Placement of the RBG, the RR, and the camera sensor relative to the FL are initially determined by application of the thin lens equation.

To demonstrate the effectiveness of the system, two experiments were performed with the density object consisting of a helium jet issuing from a small-diameter (inner diameter of 1.2 mm) stainless steel tube. For both experiments, a zoom lens with a focal length of $f = 200$ mm and an aperture setting of $f/2.8$ was used as the FL. The grid element RR consisted of a Ronchi ruling with a resolution of 1 line pair/mm. A 16-bit sCMOS camera with a resolution of 2560×2160 and 6.5 μm square pixels was used to image the helium jet. An unpolarized white 30 W LED was used as the light source. The distance between the RBG and the FL was 750 mm. The helium jet was placed approximately 368 mm from the FL, and the camera sensor plane was positioned such that the top and bottom edges of the nozzle were in sharp focus. A motorized translation stage traversed the jet along the optical axis of the instrument between the FL and the RBG. A flow-off image sequence was acquired prior to acquisition of each flow-on image sequence, and the computed average background image was then subtracted from all subsequent flow-on images.

In the first experiment, the PP was removed from the setup

to establish the minimum sensitivity of the system (essentially a bright-field schlieren). Figure 2a shows the resulting images acquired with the jet located at several positions along the optical axis relative to the position of the jet at best focus ($z = 0.0$ mm), where positive distances are closer to the RBG and negative distances are closer to the FL. In this image, the jet flow issues from the nozzle on the left-hand-side of the image and proceeds to the right. The gage pressure of helium supplied to the jet was set to 35 kPa to ensure the density object could be clearly observed, and the camera exposure was set to 10 μs. This mode of operation behaves similar to a (modified) conventional schlieren system, where a knife-edge would be located above and below the light source image (just beyond the point of any cutoff), and dark regions appear where any refractive index gradients are present. As the jet is moved away from the focal plane ($\pm z$), both the sharpness and signal magnitude of the imaged helium jet are reduced. Images in Fig. 2b were acquired at the same conditions/positions as images in Fig. 2a, but now with 152.4 mm square, 6.25 mm thick clear acrylic windows placed orthogonal to the optical axis, offset by a small distance (approximately 12.7-25.4 mm) from the flow-facing surfaces of the RBG and FL. No glare from the window back-reflections was observed in the images, and only a slight decrease in signal-to-noise occurred.

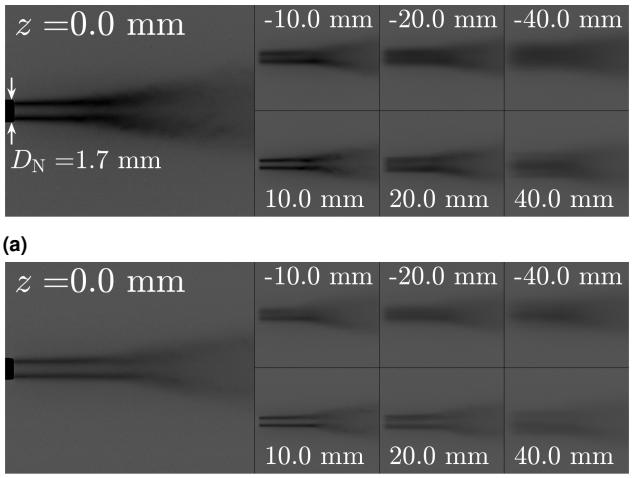

Fig. 2. Baseline focusing schlieren images of a helium jet (without the PP installed) at several positions relative to the focal plane both (a) without and (b) with windows placed in the field-of-view. The camera exposure is 10 μs, and the nozzle outer diameter is $D_{\mathrm{N}} = 1.7$ mm.

In the second experiment, a quartz Rochon prism with a beam divergence angle of 0.5° was used as the PP. Note that alternative polarizing prisms can be used as the PP (tests with a quartz Wollaston prism have produced similar results). The degree of cutoff, and therefore the sensitivity, was controlled by moving the PP either towards (less sensitivity) or away from (more sensitivity) the RR. For this particular PP and RR combination, the PP could be positioned up to approximately 30 mm from the RR, which corresponded to full cutoff. Note that changes in the resolution of the RR and divergence angle of the PP will change the distance the PP must be adjusted to in order to achieve full cutoff. The Rochon prism used as the PP in this work was oriented correctly for the projected beam. That is, the projected *lvp*-beam passed through the Rochon prism unrefracted (entrance face to exit face), and created a sharp image of the RR on the RBG. The reflected beam passed in the reverse direction through the Rochon prism (exit face to entrance face), and due to the optical activity and dispersion of the quartz material, was split into both a *lvp*-beam and an *lhp*-beam [10]. The *lvp*-beam passed unrefracted through the Rochon prism, through the RR, and was reflected out of the instrument by the PBS. The *lhp*-beam was refracted at a 0.5° angle, passed through the RR (now acting as the cutoff grid), and passed through the PBS. The camera exposure was increased to 100 μs to account for two things: the deliberate cutoff amount decreases the mean intensity, and the non-ideal operation through the quartz Rochon prism reduces the overall light throughput. While operation with the Rochon prism reduces the intensity of the light, the system still operates as intended as a focusing schlieren system. One benefit of using this Rochon prism, however, is that the use of the QWP is not strictly necessary, as the prism produces both polarization states with only the *lhp*-beam contributing to the final focused schlieren image.

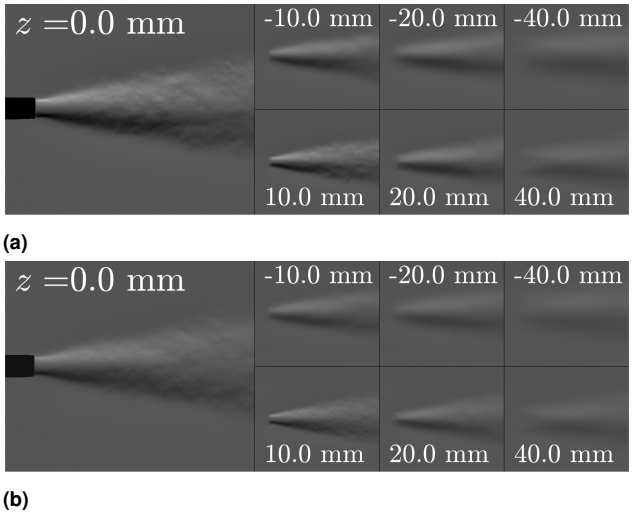

Fig. 3. Focusing schlieren images of a helium jet acquired (with the PP installed) at several positions relative to the focal plane both (a) without and (b) with windows placed in the field-of-view. The camera exposure is 100 μs, and the nozzle outer diameter is $D_{\mathrm{N}} = 1.7$ mm.

Figure 3a shows the resulting focused schlieren images acquired with the jet located at several z locations and with the Rochon prism serving as the PP. The gage pressure of helium supplied to the jet was increased to 69 kPa to generate small, yet distinct, turbulent structures. Here, as with a conventional schlieren system with the knife-edge providing approximately 50% cutoff, both light and dark intensity regions are observed corresponding to the position of refractive index gradients in the jet flow. The smaller turbulent structures away from the nozzle exit are clearly visible and attest to the system's sensitivity. Again, as the jet is scanned away from the focal plane, both the sharpness and signal magnitude of the jet flow are reduced. In Fig. 3b, the clear acrylic windows were again placed directly in front of the RBG and the FL, and again, no glare from window back-reflections was observed and only a slight reduction in signal-to-noise occurred.

In summary, a novel compact, self-aligned focusing schlieren system has been proposed that eliminates the need for a sep-

arate source grid and cutoff grid. A single grid element was projected onto a retroreflective background, and the reflection then imaged back on the original grid to provide sensitivity to a density object. The addition of a polarizing prism (in this example a Rochon prism) provided an additional offset between the imaged projection and the grid element, and the sensitivity of the system could be adjusted by moving the prism relative to the grid. A baseline level of sensitivity to the density object was demonstrated by simply re-imaging the projected grid onto the original grid element. Preliminary images obtained from a helium jet showed that images obtained with this focusing schlieren system could clearly resolve sub-millimeter scale turbulent structures with relatively high contrast and narrow focusing capability. The images were further shown to only minimally decrease in signal-to-noise when acrylic windows were placed normal to the optical axis, demonstrating the utility of this system for wind tunnel measurements.

FUNDING

National Aeronautics and Space Administration Plume Surface Interaction (PSI) Project and Transformational Tools and Technologies (TTT) Project.

DISCLOSURES

BFB and JMW: (P) Patent pending.

REFERENCES

1. G. S. Settles, *Schlieren and Shadowgraph Techniques* (Springer Berlin Heidelberg, 2001).
2. L. M. Weinstein, AIAA J. **31**, 1250 (1993).
3. L. M. Weinstein, The Eur. Phys. J. Special Top. **182**, 65 (2010).
4. J. T. Heineck, "Retroreflection Focusing Schlieren System," (1996). US Patent 5,515,158.
5. A. F. Fagan, D. L'Esperance, and K. B. Zaman, "Application of a Novel Projection Focusing Schlieren System in NASA Test Facilities," in *AIAA Aviation Forum,* (2014). Paper 2014-2522.
6. B. D. Buckner, J. D. Trolinger, and D. L'Esperance, "Digital focusing schlieren imaging," in *SPIE Optical Engineering + Applications,* (2015).
7. D. L'Esperance and B. D. Buckner, "Focusing schlieren systems usingdigitally projected grids," in *SPIE Optical Engineering + Applications,* (2017). Paper 10373-26.
8. B. D. Buckner and D. L'Esperance, "Schlieren unwrapped: distortion correction in digital focusing schlieren," in *SPIE Optical Engineering + Applications,* (2019). Paper 11102-26.
9. MetroLaser Inc., "http://www.metrolaserinc.com/technologies/high-speed-schlieren/," Online.
10. Optical Society of America, *Handbook of Optics, Vol. 2: Devices, Measurements, and Properties* (McGraw-Hill, New York, 1995), 2nd ed.

FULL REFERENCES

1. G. S. Settles, *Schlieren and Shadowgraph Techniques* (Springer Berlin Heidelberg, 2001).
2. L. M. Weinstein, "Large-Field High-Brightness Focusing Schlieren System," AIAA J. **31**, 1250–1255 (1993).
3. L. M. Weinstein, "Review and update of lens and grid schlieren and motion camera schlieren," The Eur. Phys. J. Special Top. **182**, 65–95 (2010).
4. J. T. Heineck, "Retroreflection Focusing Schlieren System," (1996). US Patent 5,515,158.
5. A. F. Fagan, D. L'Esperance, and K. B. Zaman, "Application of a Novel Projection Focusing Schlieren System in NASA Test Facilities," in *AIAA Aviation Forum,* (2014). Paper 2014-2522.
6. B. D. Buckner, J. D. Trolinger, and D. L'Esperance, "Digital focusing schlieren imaging," in *SPIE Optical Engineering + Applications,* (2015).
7. D. L'Esperance and B. D. Buckner, "Focusing schlieren systems usingdigitally projected grids," in *SPIE Optical Engineering + Applications,* (2017). Paper 10373-26.
8. B. D. Buckner and D. L'Esperance, "Schlieren unwrapped: distortion correction in digital focusing schlieren," in *SPIE Optical Engineering + Applications,* (2019). Paper 11102-26.
9. MetroLaser Inc., "http://www.metrolaserinc.com/technologies/high-speed-schlieren/," Online.
10. Optical Society of America, *Handbook of Optics, Vol. 2: Devices, Measurements, and Properties* (McGraw-Hill, New York, 1995), 2nd ed.